Supplemental material: Extracting the gravitational recoil from black hole merger signals

Vijay Varma,[1,*] Maximiliano Isi,[2,†] and Sylvia Biscoveanu[2,‡]

[1] *TAPIR 350-17, California Institute of Technology, 1200 E California Boulevard, Pasadena, CA 91125, USA*
[2] *LIGO Laboratory, Massachusetts Institute of Technology, Cambridge, Massachusetts 02139, USA*

A. Implications for tests of general relativity

At leading order, the kick's effect on the GW signal can be described as a Doppler shift of the GW frequency f [1]. Because general relativity lacks any intrinsic length scales, a uniform increase in signal frequency is completely degenerate with a decrease in total mass M, and vice versa. Thus, if not explicitly accounted for, a frequency shift due to a kick will bias mass measurements. This is analogous to the effect of the cosmological redshift z on the GWs: GW measurements only measure the combination $M(1+z)$ known as the detector-frame mass, and the source-frame mass is only inferred after assuming a cosmology [2]. One important difference between the cosmological and kick redshifts is that, in the latter, the Doppler shift occurs only when the kick is imparted, mostly near the merger [3–6]. Therefore the Doppler shift only affects the merger and ringdown part of the signal, while a cosmological redshift rescales the GW signal as a whole.

The amount of Doppler shift depends on the projection of the kick velocity along the line of sight. At leading order, the Doppler-shifted remnant mass is given by [1]:

$$m_f^{\rm DS} = m_f\,(1 + \boldsymbol{v}_f \cdot \hat{\boldsymbol{n}}/c), \tag{S1}$$

where c is the speed of light and $\hat{\boldsymbol{n}}$ is the unit vector pointing from the observer to the source. From our inference setup, we obtain posterior distributions for the component parameters $\boldsymbol{\Lambda} = \{m_1, m_2, \boldsymbol{\chi}_1, \boldsymbol{\chi}_2\}$, as well as the line-of-sight parameters $(\iota, \phi_{\rm ref})$. Our method to measure the kick recovers the full kick vector $\boldsymbol{v}_f$ given $\boldsymbol{\Lambda}$. For each posterior sample, we then project the kick along the line of sight to obtain the Doppler-shifted remnant mass.

The Doppler shift due to the kick velocity can play an important role in tests of general relativity using the ringdown signal [7–16]. In some of these tests, the remnant mass and spin are measured from different portions of the signal and compared against each other to check for consistency. In one version of the test, the full inspiral-merger-ringdown signal is first analyzed using a waveform model and posterior distributions are obtained for $\boldsymbol{\Lambda}$. These are then passed to fitting formulae (e.g. [17–21]) for the remnant mass and spin to obtain posterior distributions for these quantities. Finally, considering only the ringdown signal and varying the quasi-normal-mode frequencies [22–25], the remnant mass and spin are independently measured [7, 8, 10, 13–15].

In the first case the inferred remnant mass is not sensitive to the Doppler shift as traditional fitting formulas for the remnant mass do not account for this. Apart from modeling errors, this is equivalent to measuring the remnant mass from the apparent horizon of the remnant black hole in an NR simulation [26]. In the second case, however, the observed ringdown frequencies would be Doppler-shifted and the inferred remnant mass would be the Doppler-shifted value. For large Doppler shifts, these two measurements of the remnant mass would be inconsistent, mimicking a deviation from general relativity.

Fig. 6 in the main document shows the remnant mass posterior distribution before and after the Doppler shift for the superkick configuration of Fig. 3. The `NRSur7dq4Remnant` model is used to predict the kick vector and the remnant mass before the Doppler shift, while Eq. (S1) is used to predict the Doppler-shifted remnant mass. The two mass distributions are visibly different in Fig. 6, therefore this will be important to account for in ringdown tests of general relativity. However, this is a fairly fine-tuned source configuration with a large kick velocity. This effect is expected to become important when the measurement precision for the remnant mass is comparable or smaller than the Doppler shift, $\delta m_f/m_f \lesssim |\boldsymbol{v}_f \cdot \hat{\boldsymbol{n}}/c|$. Unless signals with kick magnitudes of order 1000 km/s are detected, we expect that this effect will only be important for third-generation GW detectors. In any case, our method can already be used to account for this effect in tests of general relativity.

B. Probability-Probability plots

To demonstrate the robustness of our Bayesian inference infrastructure using the `NRSur7dq4` and `NRSur7dq4Remnant` models, we produce a probability-probability (P-P) plot for the kick velocity, from a set of 87 simulated binary BH injections into design-sensitivity Gaussian noise for a LIGO Hanford-Livingston-Virgo detector network. (See, e.g. Ref. [27] for an example of P-P plots in the context of GW data analysis.) For each injection, we run the LALInference parameter estimation package [28] to obtain posteriors for the binary parameters, like the masses and spins ($\boldsymbol{\Lambda}$). From those, we then derive posteriors on the kick parameters using the `NRSur7dq4Remnant` surrogate. The P-P plot shows the fraction of events for which the posterior for a given

* vvarma@caltech.edu
† maxisi@mit.edu; NHFP Einstein fellow
‡ sbisco@mit.edu

parameter recovers the true value at a particular credible interval, as a function of the credible interval. If the posteriors are sampled successfully, the P-P plot should be diagonal—meaning that the true value is recovered within the x%-credible interval x% of the time, consistent with statistical error.

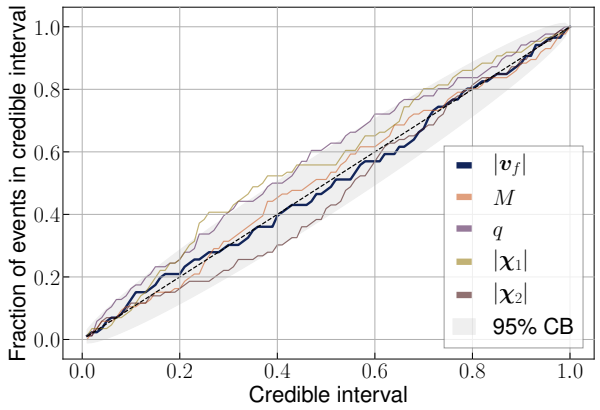

Figure S1. P-P plot for 87 binary black hole injections into design sensitivity Gaussian noise recovered with the `NRSur7dq4` and `NRSur7dq4Remnant` models for the kick magnitude, as well as the total mass, mass ratio, and spin magnitudes. The diagonal is shown in the black dashed line along with the 95% confidence band (CB) in the shaded gray.

We draw the 87 injections from a distribution uniform in component masses m_1, m_2 between 18 and 110 $M_\odot$, but restricted to a mass ratio of $q = m_1/m_2 \leq 3$ and total mass $M \geq 72\,M_\odot$. The spin magnitudes are drawn uniformly between $0 \leq |\boldsymbol{\chi}_1|, |\boldsymbol{\chi}_2| \leq 0.8$, and the directions are distributed isotropically on a sphere. The luminosity distances are picked with a density proportional to their square (that is, uniform in volume) out to 5 Gpc, and the inclination angle is drawn from a uniform-in-cosine distribution. The location of the source in the sky is drawn isotropically, as is its polarization angle. The same distributions are used as the priors during the parameter estimation step.

The P-P plot for the 87 simulated injections is shown in Fig. S1. We display the distributions for the kick magnitude ($|\boldsymbol{v}_f|$), total mass (M), mass ratio (q), and component spin parameters $|\boldsymbol{\chi}_1|, |\boldsymbol{\chi}_2|$, which all lie largely within the 95% confidence band around the diagonal (shaded in gray). The p-value for the probability that the fraction of events within a given credible interval for the kick magnitude is drawn from uniform distribution between 0 and 1, as expected for a diagonal P-P plot, is 98.6%. This demonstrates that the kick posteriors generated with `NRSur7dq4Remnant`, in combination with the LALINFERENCE sampler, are statistically robust and behave as expected in simulated Gaussian noise. Deviations between the true value and the peak of the recovered posterior, such as those seen in Fig. 4, are consistent with statistical fluctuations.

C. Prior distribution for component parameters

Analyses presented in the main text, for both injections and real data, use similar priors to those described in Sec. B. This choice follows standard conventions for LIGO-Virgo analyses (e.g., see Appendix C in [29]). We vary the specific mass ranges allowed to ensure the posterior always has full support within the prior. For injections, the prior was uniform in component masses m_1, m_2 between 10 and 120 $M_\odot$, but restricted to mass ratios $q = m_1/m_2 \leq 4$ and total masses $M \geq 60\,M_\odot$. The spin magnitudes are drawn uniformly between $0 \leq |\boldsymbol{\chi}_1|, |\boldsymbol{\chi}_2| \leq 0.99$, and the directions are distributed isotropically on a sphere. The priors on the extrinsic parameters are the same as in Sec. B.

[1] Davide Gerosa and Christopher J. Moore, "Black hole kicks as new gravitational wave observables," Phys. Rev. Lett. **117**, 011101 (2016), arXiv:1606.04226 [gr-qc].

[2] A Krolak and Bernard F Schutz, "Coalescing binaries—Probe of the universe," General Relativity and Gravitation **19**, 1163–1171 (1987).

[3] Jose A. Gonzalez, Ulrich Sperhake, Bernd Bruegmann, Mark Hannam, and Sascha Husa, "Total recoil: The Maximum kick from nonspinning black-hole binary inspiral," Phys. Rev. Lett. **98**, 091101 (2007), arXiv:gr-qc/0610154 [gr-qc].

[4] Carlos O. Lousto and Yosef Zlochower, "Further insight into gravitational recoil," Phys. Rev. **D77**, 044028 (2008), arXiv:0708.4048 [gr-qc].

[5] Carlos O. Lousto, Yosef Zlochower, Massimo Dotti, and Marta Volonteri, "Gravitational Recoil From Accretion-Aligned Black-Hole Binaries," Phys. Rev. **D85**, 084015 (2012), arXiv:1201.1923 [gr-qc].

[6] Carlos O. Lousto and Yosef Zlochower, "Nonlinear Gravitational Recoil from the Mergers of Precessing Black-Hole Binaries," Phys. Rev. **D87**, 084027 (2013), arXiv:1211.7099 [gr-qc].

[7] Olaf Dreyer, Bernard J. Kelly, Badri Krishnan, Lee Samuel Finn, David Garrison, and Ramon Lopez-Aleman, "Black hole spectroscopy: Testing general relativity through gravitational wave observations," Class. Quant. Grav. **21**, 787–804 (2004), arXiv:gr-qc/0309007 [gr-qc].

[8] S. Gossan, J. Veitch, and B. S. Sathyaprakash, "Bayesian model selection for testing the no-hair theorem with black hole ringdowns," Phys. Rev. **D85**, 124056 (2012), arXiv:1111.5819 [gr-qc].

[9] J. Meidam, M. Agathos, C. Van Den Broeck, J. Veitch, and B. S. Sathyaprakash, "Testing the no-hair theorem with black hole ringdowns using TIGER," Phys. Rev. **D90**, 064009 (2014), arXiv:1406.3201 [gr-qc].

[10] B. P. Abbott *et al.* (LIGO Scientific, Virgo), "Tests of general relativity with GW150914," Phys. Rev. Lett. **116**, 221101 (2016), [Erratum: Phys. Rev. Lett.121,no.12,129902(2018)], arXiv:1602.03841 [gr-qc].

[11] B. P. Abbott *et al.* (LIGO Scientific, Virgo), "Tests of General Relativity with the Binary Black Hole Signals from the LIGO-Virgo Catalog GWTC-1," Phys. Rev. **D100**, 104036 (2019), arXiv:1903.04467 [gr-qc].

[12] Abhirup Ghosh, Nathan K. Johnson-Mcdaniel, Archisman Ghosh, Chandra Kant Mishra, Parameswaran Ajith, Walter Del Pozzo, Christopher P. L. Berry, Alex B. Nielsen, and Lionel London, "Testing general relativity using gravitational wave signals from the inspiral, merger and ringdown of binary black holes," Class. Quant. Grav. **35**, 014002 (2018), arXiv:1704.06784 [gr-qc].

[13] Richard Brito, Alessandra Buonanno, and Vivien Raymond, "Black-hole Spectroscopy by Making Full Use of Gravitational-Wave Modeling," Phys. Rev. **D98**, 084038 (2018), arXiv:1805.00293 [gr-qc].

[14] Gregorio Carullo, Walter Del Pozzo, and John Veitch, "Observational Black Hole Spectroscopy: A time-domain multimode analysis of GW150914," Phys. Rev. **D99**, 123029 (2019), [Erratum: Phys. Rev.D100,no.8,089903(2019)], arXiv:1902.07527 [gr-qc].

[15] Maximiliano Isi, Matthew Giesler, Will M. Farr, Mark A. Scheel, and Saul A. Teukolsky, "Testing the no-hair theorem with GW150914," Phys. Rev. Lett. **123**, 111102 (2019), arXiv:1905.00869 [gr-qc].

[16] Matthew Giesler, Maximiliano Isi, Mark Scheel, and Saul Teukolsky, "Black hole ringdown: the importance of overtones," Phys. Rev. **X9**, 041060 (2019), arXiv:1903.08284 [gr-qc].

[17] Enrico Barausse, Viktoriya Morozova, and Luciano Rezzolla, "On the mass radiated by coalescing black-hole binaries," Astrophys. J. **758**, 63 (2012), [Erratum: Astrophys. J.786,76(2014)], arXiv:1206.3803 [gr-qc].

[18] Fabian Hofmann, Enrico Barausse, and Luciano Rezzolla, "The final spin from binary black holes in quasi-circular orbits," Astrophys. J. **825**, L19 (2016), arXiv:1605.01938 [gr-qc].

[19] Xisco Jiménez-Forteza, David Keitel, Sascha Husa, Mark Hannam, Sebastian Khan, and Michael Pürrer, "Hierarchical data-driven approach to fitting numerical relativity data for nonprecessing binary black holes with an application to final spin and radiated energy," Phys. Rev. **D95**, 064024 (2017), arXiv:1611.00332 [gr-qc].

[20] James Healy and Carlos O. Lousto, "Remnant of binary black-hole mergers: New simulations and peak luminosity studies," Phys. Rev. **D95**, 024037 (2017), arXiv:1610.09713 [gr-qc].

[21] James Healy, Carlos O. Lousto, and Yosef Zlochower, "Remnant mass, spin, and recoil from spin aligned black-hole binaries," Phys. Rev. **D90**, 104004 (2014), arXiv:1406.7295 [gr-qc].

[22] C. V. Vishveshwara, "Stability of the schwarzschild metric," Phys. Rev. D **1**, 2870–2879 (1970).

[23] William H. Press, "Long Wave Trains of Gravitational Waves from a Vibrating Black Hole," Astrophysical Journal **170**, L105 (1971).

[24] Saul A. Teukolsky, "Perturbations of a Rotating Black Hole. I. Fundamental Equations for Gravitational, Electromagnetic, and Neutrino-Field Perturbations," Astrophysical Journal **185**, 635–648 (1973).

[25] S. Chandrasekhar and S. Detweiler, "The quasi-normal modes of the schwarzschild black hole," Proceedings of the Royal Society of London. Series A, Mathematical and Physical Sciences **344**, 441–452 (1975).

[26] Michael Boyle *et al.*, "The SXS Collaboration catalog of binary black hole simulations," Class. Quant. Grav. **36**, 195006 (2019), arXiv:1904.04831 [gr-qc].

[27] Jonathan R. Gair and Christopher J. Moore, "Quantifying and mitigating bias in inference on gravitational wave source populations," Phys. Rev. **D91**, 124062 (2015), arXiv:1504.02767 [gr-qc].

[28] J. Veitch *et al.*, "Robust parameter estimation for compact binaries with ground-based gravitational-wave observations using the LALInference software library," Phys. Rev. D **91**, 042003 (2015), arXiv:1409.7215 [gr-qc].

[29] B. P. Abbott *et al.* (LIGO Scientific, Virgo), "GWTC-1: A Gravitational-Wave Transient Catalog of Compact Binary Mergers Observed by LIGO and Virgo during the First and Second Observing Runs," Phys. Rev. **X9**, 031040 (2019), arXiv:1811.12907 [astro-ph.HE].